J. Fluid Mech. (1967), *vol.* 30, *part* 2, *pp.* 337–355
Printed in Great Britain

Heat transfer from a circular cylinder by acoustic streaming

By PETER D. RICHARDSON
Division of Engineering, Brown University, Providence, R.I. 02912

(Received 7 March 1967)

An analysis is described for convection from a circular cylinder subjected to transverse oscillations relative to the fluid in which it is immersed. The analysis is based upon use of the acoustic streaming flow field. It is assumed that the frequency involved is sufficiently small that the acoustic wavelength in the fluid is much larger than the cylinder diameter, and that there is no externally imposed mean flow across or along the cylinder. Solutions are presented which are appropriate for a wide range of Prandtl number, and the cases of small and of large streaming Reynolds number are distinguished. The analysis compares favourably with experiments when the influence of natural convection is small.

1. Introduction

Substantial improvements in such processes as heat exchange, sublimation, drying, dissolution and so on have been brought about by the use of pulsations or vibrations imposed upon the fluid. Investigations intended to clarify the mechanisms by which the improvements are brought about have led to conflicting conclusions. A review of the subject was given recently by Richardson (1967). It has become clear that there is no single, universal explanation which can be invoked, but that there are a few distinguishable mechanisms. One of the configurations which has been used extensively in experiments is that of a horizontal circular cylinder immersed in a fluid. Studies have been made with relative oscillations between the cylinder and the fluid in both the axial direction of the cylinder and transversely to the cylinder. In this paper, attention is concentrated upon the effects of oscillations which are transverse to the cylinder. Further, consideration is restricted to the cases where no flow occurs in the absence of vibrations or oscillations except that caused by natural convection.

It has been known for many years that oscillating flows can generate steady, secondary flows in the vicinity of solid surfaces. The first mathematical solution of the problem of streaming motion around a circular cylinder was obtained by Schlichting (1932) by techniques of laminar boundary-layer theory. This solution predicted that there would be two distinct regions of streaming in each quadrant around the cylinder; this consists of one region next to the cylinder (sometimes called the d.c. boundary layer), and an outer streaming in the region radially further from the axis. The form of the motion is illustrated in a streamline diagram in figure 1 for horizontal oscillation of a circular cylinder in an infinite

fluid. For the purpose of illustration, the inner streaming region has been exaggerated in size. In Schlichting's analysis the d.c. boundary-layer thickness is proportional to the a.c. boundary-layer thickness, $(\nu/\omega)^{\frac{1}{2}}$, sometimes designated as $\delta_{\text{a.c.}}$. It is to be noted that this length scale is independent of the amplitude of oscillation, and depends solely upon the transport properties of the fluid and the

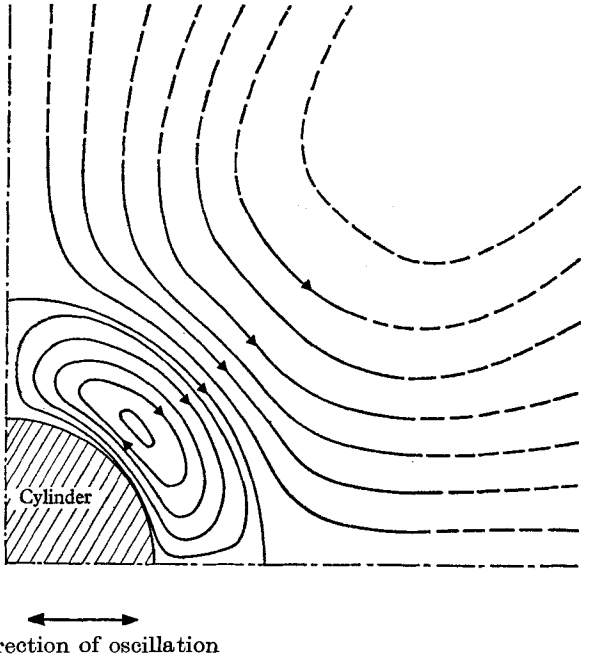

FIGURE 1. Streamlines of the steady streaming motion induced by transverse oscillations of a circular cylinder. The inner and outer streaming motions have opposite rotation. The radial extent of the inner streaming has been greatly exaggerated from the typical scale in boundary-layer flow so that the motion can be seen clearly.

frequency of oscillation. When the frequency of oscillation is reduced, or the kinematic viscosity of the fluid is increased, so that the a.c. boundary-layer thickness exceeds about one-tenth of the cylinder diameter, it is no longer appropriate to analyse the flow with laminar boundary-layer theory and the full Navier–Stokes equations must be used. An analysis of the flow of this type was presented by Holtsmark, Johnson, Sikkeland & Skavlem (1954), who showed that the flow field was qualitatively similar to that obtained by boundary-layer theory with the directions of streaming maintained in the same sense in each quadrant, but in which the inner streaming layer became larger than predicted by boundary-layer theory and in which the streaming velocities were also notably greater. An experimental investigation by Raney, Corelli & Westervelt (1954) showed that the size of the inner streaming layer departed systematically from the values predicted by laminar boundary-layer theory as the ratio of the a.c. boundary-layer thickness to the cylinder diameter was increased. In these investigations of the secondary motion known as acoustic streaming, analysis

and experiment alike were restricted to the situations where no heat or mass transfer occurs from the cylinder.

Some evidence has been presented which supports qualitatively the hypothesis of convection by acoustic streaming. In a recent series of observations of local heat transfer, Richardson (1964, 1966) found that, with a horizontal heated cylinder placed in horizontal and vertical transverse standing sound fields, local changes in heat transfer occur when the sound intensity is well below that for which significant changes in overall transfer have been found. The local changes were in different directions at different locations around the cylinder and the corresponding overall change was small enough to have gone unnoticed in the earlier studies on overall heat transfer determined by energy balance techniques.

It is the purpose of this paper to discuss the mechanics of convection from a heated cylinder subjected to transverse oscillations or placed in a sound field, to present an analysis for convection by ordinary acoustic streaming and to show that there is promising agreement with the appropriate experimental results.

2. The fluid motion in perspective

It is possible to obtain acoustic wavelengths which are large or small compared with the diameter of the cylinder, by choice of the fluid in which a cylinder is immersed and of the frequency of oscillation. The discussion here is restricted to those circumstances in which the wavelength is large compared with the diameter of the cylinder.

The oscillations can be described, in part, in terms of the ratio of the displacement amplitude of the oscillation to the cylinder diameter. It is possible to have oscillations in which the displacement amplitude is very small compared with the cylinder diameter, so that in the primary flow there is no regular systematic displacement of the fluid across the cylinder in such a way that the convection of heat from the cylinder has an obvious 'vehicle'. However, as noted earlier, there arises in such situations a steady, secondary flow by means of which regular convection currents pass over the surface of the cylinder and are able to effect a net transfer of enthalpy from the region immediately surrounding the cylinder. For cases of practical interest it is irrelevant whether the cylinder is held stationary and the fluid oscillated relative to it (by creation of a velocity antinode in a standing sound field), or vice versa. Analytically it can be shown that the two cases are equivalent when the fluid is incompressible.

Unfortunately, experimental results are complicated by the presence of buoyancy effects. In practical terms, the influence of natural convection can be so great that the oscillations are felt as little more than a perturbation upon the natural convection flow except at very high intensities. This fact considerably confuses the picture when experimental results are examined, and it is necessary to introduce a further dimensionless parameter by which the relative significance of natural convective forces to the forced convection associated with the oscillations can be measured. A suitable dimensionless parameter is a ratio of the Grashof number to the square of the Reynolds number. It is common experience

in the accounting of convection that measurements tend to correspond to analysis in which natural convective effects are neglected in the limit as the ratio tends to zero, and it will be found that this experience is repeated here.

The measurements which have been made span large ranges of the dimensionless variables a/d and $(\nu/\omega)^{\frac{1}{2}}/d$. The results of measurements where $a/d > 1$ can be accounted for satisfactorily on the basis of expressions used to represent heat transfer under the corresponding steady conditions. It is on the data for measurements with $a/d \ll 1$ that attention must be concentrated, since it is for these that no satisfactory accounting has yet been made. It is shown below that ordinary acoustic streaming plays a dominant role in this.

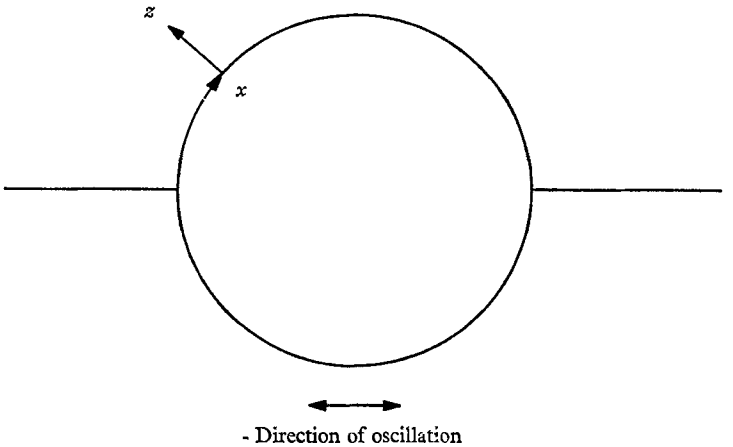

FIGURE 2. Co-ordinate system on the cylinder for calculation of the isothermal acoustic streaming at small streaming Reynolds numbers. Similar co-ordinates are used in other calculations, except that the origin for x is taken at the forward stagnation point for the relevant flow.

It is necessary first to discuss some details of the fluid motion. For the present work, the case of progressive sound fields is excluded, and it is considered that the cylinder is either at a velocity antinode of a transverse standing sound field or is oscillated transversely. The basic boundary-layer analysis for periodic flows in the absence of a mean flow, following Schlichting (1932), has been described in several books; the most extensive discussion was given by Stuart (1963) in a recent Fluid Motion Memoir (Rosenhead 1963). It can be shown that if $(\delta_{\text{a.c.}}/d)$ is small, and also $U_\infty/\omega d$ is small (where $U_\infty \cos \omega t$ is the instantaneous relative velocity of cylinder and fluid) then the first-order oscillatory motion and the second-order steady streaming motion can be calculated from the unsteady boundary-layer approximation of the Navier–Stokes equations. The co-ordinate system is illustrated in figure 2. The first term in the stream function can be written

$$\psi_1 = (2\nu/\omega)^{\frac{1}{2}} U_0(x) f_1(\eta) \exp(i\omega t), \tag{1}$$

where $U_0(x)$ is the velocity outside the boundary layer and locally parallel to the wall of the cylinder, $\eta = z(\omega/2\nu)^{\frac{1}{2}}$, and

$$f_1(\eta) = -\tfrac{1}{2}(1-i)[1-\exp(-(1+i)\eta)]+\eta. \tag{2}$$

The second term in the stream function involves terms of zero frequency and of a frequency twice that of the primary flow. The second term can be written

$$\psi_2 = \left(\frac{2\nu}{\omega}\right)^{\frac{1}{2}} \frac{U_0}{\omega}\frac{dU_0}{dx}(f_{20}+f_{22}\exp(2i\omega t)). \tag{3}$$

When this is substituted into the boundary-layer equation, and the known result for ψ_1 is introduced, a solution for the steady streaming can be found

$$f_{20} = \tfrac{1}{8}^3 - \tfrac{3}{4}\eta - \tfrac{1}{8}e^{-2\eta} - \tfrac{3}{2}e^{-\eta}\cos\eta - e^{-\eta}\sin\eta - \tfrac{1}{2}\eta\, e^{-\eta}\sin\eta, \tag{4}$$

which satisfies the boundary conditions

$$\left.\begin{aligned} &f_{20} = f'_{20} = 0 \quad \text{at} \quad \eta = 0, \\ &f'_{20} \quad \text{remains finite as} \quad \eta \to \infty. \end{aligned}\right\} \tag{5}$$

At large values of η, $f'_{20} = -\frac{3}{4}$, and this demonstrates that there is a flow outside the boundary layer and locally parallel to the surface of velocity

$$u = -\frac{3}{4}\frac{U_0}{\omega}\frac{dU_0}{dx}. \tag{6}$$

This velocity plays an important role in the analysis of thermal convection. There is also a steady component of velocity normal to the surface, given by

$$w = \frac{1}{\omega}\frac{d}{dx}\left(U_0\frac{dU_0}{dx}\right)\left\{\frac{3}{4}z - \frac{13}{8}\left(\frac{2\nu}{\omega}\right)^{\frac{1}{2}}\right\}. \tag{7}$$

This has maxima and minima at the boundaries of the four quadrants, as illustrated in figure 1. In these positions the flow exterior to the boundary layer is very similar to that found at ideal forward or rearward stagnation points.

The secondary motion is generated by the Reynolds stress associated with the primary boundary-layer flow. The magnitude of the secondary flow is independent of the viscosity, and is of order $U_\infty^2/\omega d$, which can be used to form a streaming Reynolds number, $Re_s = U_\infty^2/\omega\nu$. Stuart pointed out that the original solutions are pertinent when this streaming Reynolds number is small, but that when the streaming Reynolds number becomes large a second boundary layer develops, at the edge of which the steady velocity component tends to zero. The thickness of this second boundary layer, δ_{outer}, is such that

$$\delta_{\text{a.c.}}/\delta_{\text{outer}} = O(a/d). \tag{8}$$

Measurements which have been made in sound fields in air, together with Martinelli & Boetler's (1938) measurements for a cylinder oscillating in water, are all for $a/d \ll 1$ so that the flow field in the absence of natural convection should be described adequately by the analysis above, equations (1)–(7). For cylinders vibrated in air at lower frequencies (yet still within the range of boundary-layer theory) it becomes necessary for this outer layer to be taken into account.

3. Heat transfer by acoustic streaming

The analysis of thermal transport by the flow described above can also be based upon boundary-layer theory. It is commonly possible to analyse laminar transport from isothermal surfaces by noting that, for a given body, the thermal

boundary-layer thickness and the velocity boundary-layer thickness are in constant proportion to each other, and their ratio is related to the Prandtl number, Pr, of the fluid. For the two cases where one layer is very large compared with the other, it is possible to use simple approximations for the flow field and thereby obtain quickly two asymptotic solutions for $Pr \to 0$ and $Pr \to \infty$. The situation for the present problem is not quite as simple, since there are two velocity boundary-layer thicknesses to consider: the inner streaming motion thickness, which is of the same order as the a.c. boundary-layer thickness and which does not change with change in the oscillation amplitude, and the outer streaming thickness which decreases as the amplitude increases.

For some cases of interest in the present investigation, the outer streaming layer is large enough to be considered infinite in size: then the only comparison to be made is between the thermal boundary layer and the inner streaming layer. It is reasonable to expect that the former will decrease in thickness as the amplitude increases, so that the ratio of boundary-layer thicknesses will not be constant (the positions where the streaming motion is directed radially outward are excluded from consideration for the present). Thus, when the amplitude of oscillation is small, the thermal boundary layer is large compared with the inner streaming layer, a situation more normally encountered when the Prandtl number is small. Here, however, it can occur even for $Pr > 1$. The convection process is dominated by the outer streaming motion, and can be computed using techniques normally appropriate for $Pr \to 0$.

If the real Prandtl number is very large, the thermal boundary layer is small and decreases in size with increase in intensity; for sufficiently large amplitudes the thermal boundary layer is much smaller than the inner streaming motion, and convection can be computed using the normal techniques for $Pr \to \infty$. This case should present more difficulties in analysis than usual, in that heat must be transferred from the surface to the inner streaming fluid and then from the inner streaming (which has closed streamlines) to the outer streaming. Fortunately, this case can only be encountered when the real Prandtl number is very large; there are only two investigations which correspond to this, involving mass transfer at very large Schmidt numbers (Rao, Raju & Rao 1963; Jameson 1964) and these investigations were performed in a range where the a.c. boundary-layer thickness was too large to be accounted for adequately by boundary-layer theory. Some results in air, water and aqueous glycerine are also somewhat within the scope of this case, as will be noted later.

One remaining case to be considered is that where the thermal boundary-layer thickness is large compared with the inner streaming, but the outer streaming boundary layer is similar in size. Both the thermal layer and the outer boundary-layer shrink in size as the amplitude increases. Both layers vary as the inverse square root of the streaming Reynolds number, i.e. they vary inversely with the amplitude. With this situation, the boundary layers are (to a first approximation) in constant proportion to each other, independent of amplitude. For measurements made in sound fields by Fand & Kaye (1961*a*) the streaming Reynolds number rises to the order of 10, but for measurements involving vibration of cylinders (e.g. Fand & Kaye 1961*b*) the streaming Reynolds number goes

as high as about 500. This is largely a consequence of the smaller frequency in the latter case. An analysis which examines this boundary-layer flow has been developed by Stuart (1966).

Convection by outer streaming at small streaming Reynolds number

The first of the three cases to be considered for boundary-layer analysis of thermal convection is where

$$\delta_{\text{thermal}} \gg \delta_{\text{a.c.}}$$

and

$$\delta_{\text{outer}} \gg \delta_{\text{thermal}}.$$

For this case, the convection is due essentially to the outer streaming flow, in which u is given by (6). Examination of figure 1 points out that the outer streaming motion has forward stagnation points at the top and bottom of a cylinder if the primary motion is a horizontal oscillation. These points can serve as starting points for thermal boundary layers which are carried round for $\frac{1}{2}\pi$ radians to the separation points of the streaming motion. The function

$$U_0(x) = 2a\omega \sin(x/R),$$

so that the outer acoustic streaming velocity is

$$u_1 = \frac{3a^2\omega}{R} \sin\frac{x}{R} \cos\frac{x}{R}. \tag{9}$$

As noted before, with $\delta_{\text{thermal}} \gg \delta_{\text{a.c.}}$, the techniques for low Pr are to be used. It is convenient to introduce the assumption of local similarity, an assumption which has been given some weight by Meksyn (1961), Merk (1959) and others. It was shown by Evans (1962) that the conduction thickness, $\Delta_4 = k/h$, with $Pr = 0$ could be found from the equation

$$\frac{u_1}{\alpha}\frac{d\Delta_4^2}{dx} = \pi - 2\frac{\Delta_4^2}{\alpha}\frac{du_1}{dx}. \tag{10}$$

It is possible to obtain an exact solution for this. When the substitutions $D = \Delta_4 a\omega^{\frac{1}{2}}/R\alpha^{\frac{1}{2}}$, $\theta = 2x/R$ are made, and equation (9) is used, (10) becomes

$$3\sin\theta\frac{dD^2}{d\theta} = \pi - 6D^2\cos\theta. \tag{11}$$

It is obvious that (11) is satisfied by

$$D = ka\omega^{\frac{1}{2}}/hR\alpha^{\frac{1}{2}} = (\pi/6)^{\frac{1}{2}}\sec(x/R). \tag{12}$$

This means that the local heat transfer coefficient around one quadrant of a cylinder is proportional to $\cos(x/R)$, and if a polar diagram of the local transfer coefficient is constructed it resembles a 'figure eight'. This figure eight is upright if the oscillation is in the horizontal direction, as illustrated in figure 3. The figure eight will be rotated through $\frac{1}{2}\pi$, to lie on its side, if the oscillations are in the vertical direction. The average heat transfer is $2/\pi$ times the maximum, and a conventional dimensionless representation of the mean transfer rate is given by

$$\frac{\bar{h}d}{k}\Big/\left(\frac{a^2\omega}{\nu}\right)^{\frac{1}{2}} = \overline{Nu}/Re_s^{\frac{1}{2}} = \left(\frac{96}{\pi^3}\right)^{\frac{1}{2}} Pr^{\frac{1}{2}} = 1{\cdot}76Pr^{\frac{1}{2}}, \tag{13}$$

or by

$$\overline{Nu}/Re_{\text{osc}} = \left(\frac{16}{\pi^3}\right)^{\frac{1}{2}} Pr^{\frac{1}{2}}\left(\frac{3\nu}{\omega}\right)^{\frac{1}{2}}\Big/R = 0{\cdot}718Pr^{\frac{1}{2}}\left(\frac{3\nu}{\omega}\right)^{\frac{1}{2}}\Big/R. \tag{14}$$

The use of an analysis for $Pr \to 0$ has meant that the details of the streaming motion inside the d.c. boundary layer have been ignored completely. The inner streaming motion involves velocities which are less than u_1 and in the opposite

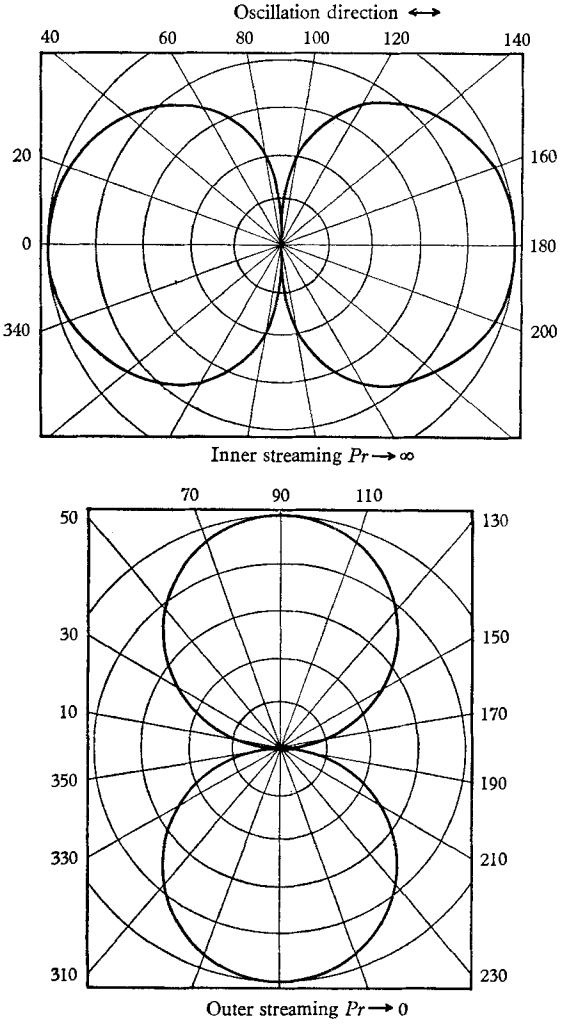

FIGURE 3. Polar graphs of the local variation of heat transfer coefficient. The associated direction of oscillation is horizontal. The maximum values occur at the forward stagnation points for the corresponding streaming motions. The azimuthal variation for inner streaming is determined from (20) and for outer streaming from (12). It can be seen that the local heat transfer is more nearly constant at positions near the forward stagnation points for the inner streaming.

direction; the maximum inner velocity is about one-seventh the magnitude of u_1. As the Reynolds number is increased, the conduction thickness Δ_4 becomes smaller, and it is necessary to take account of the inner motion. It is convenient to introduce an approximation, based on the following arguments: since the inner layer has small velocities, lies deep inside the thermal boundary layer and is very long compared to its thickness, such a layer transmits heat by pure conduction.

The inner streaming can be approximated by a pure conduction layer, the thickness of which is the thickness of the inner streaming motion (up to the dividing streamline). On the outside of this is the flow which gives, at the interface (the dividing streamline), the heat transfer coefficient determined by the analysis above. Thus the conduction layer and boundary layer form resistances to heat in series. To the order of approximation involved it is sufficient to base the correction factor on the average heat transfer coefficient, so that (13) and (14) become

$$\overline{Nu}/Re_s^{\frac{1}{2}} = 1{\cdot}76Pr^{\frac{1}{2}}/\{1+1{\cdot}66(a/d)Pr^{\frac{1}{2}}\} \tag{15}$$

and

$$\overline{Nu}/Re_{\text{osc}} = 0{\cdot}718Pr^{\frac{1}{2}}(3\nu/\omega)^{\frac{1}{2}}/R\{1+1{\cdot}66(a/d)Pr^{\frac{1}{2}}\}. \tag{16}$$

With the restriction in the fluid-mechanical analysis that $a/d \ll 1$, the correction factor should be small unless the Prandtl number is large. The largest corrections are needed in analysing the work of Martinelli & Boelter (1938) in water, but even in that case the factor does not rise above 1·5.

Convection by inner streaming

Another case to be considered in the framework of boundary-layer analysis is that of very large Prandtl numbers. In the asymptotic condition, $Pr \to \infty$, another limiting relationship should be found. It is possible to express the wall shear stress as a function of x, and to use an analysis applicable for arbitrary (but continuous) distribution of wall shear stress with $Pr \to \infty$. With this analysis the heat transfer coefficient is determined for the difference in temperature between the wall and the middle region of the inner streaming; there can be further resistance to heat transfer across the dividing streamline where the inner flow adjoins the outer flow, but this is not investigated in detail here because in the corresponding experiments $\delta_{\text{a.c.}}/d$ is not small and the interface region is much longer than the boundary layer on the wall, and each case needs to be considered on its merits. The estimation of the interface resistance will be discussed in comparison of experiments with analysis.

It is convenient to express the analysis in terms which permit inclusion of the cases where $(\delta_{\text{a.c.}}/d)$ is not small. This can be done by introducing a coefficient H into the expression for the streaming velocity gradient at the wall: H can assume a value appropriate to the corresponding $(\delta_{\text{a.c.}}/d)$. If the difference in temperature between the wall and the stream outside the thermal boundary layer is constant, and $Pr \to \infty$, the wall gradient of the dimensionless temperature Θ is

$$\left(\frac{\partial\Theta}{\partial z}\right)_0 = \frac{1}{\Gamma(\frac{4}{3})} \frac{(\partial u/\partial z)_{z=0}^{\frac{1}{3}}}{\left\{9\alpha \int_0^x (\partial u/\partial z)_0^{\frac{1}{3}} dx\right\}^{\frac{1}{3}}}. \tag{17}$$

This is clearly the reciprocal of the conduction thickness, Δ_4, as considered in the previous case. From equation (4), with the factor H introduced, the velocity gradient at the surface is

$$\left(\frac{\partial u}{\partial z}\right)_{z=0} = H\frac{\omega a^2}{R}\left(\frac{\omega}{2\nu}\right)^{\frac{1}{2}} \sin\left(\frac{2x}{R}\right). \tag{18}$$

The x-dependence in (17) can be expressed as

$$\frac{\sin^{\frac{1}{2}}\theta}{\left\{\int_0 \sin^{\frac{1}{2}}\theta\, d\theta\right\}^{\frac{1}{3}}}. \tag{19}$$

The indefinite integral can be reduced to a tabulated function by the substitution $p = \sin^2\theta$, by which (19) becomes

$$2^{\frac{1}{3}}\sin^{\frac{1}{2}}\theta \Big/ \left\{\int_0 p^{-\frac{1}{4}}(1-p)^{-\frac{1}{2}}\, dp\right\}^{\frac{1}{3}} = 2^{\frac{1}{3}}\sin^{\frac{1}{2}}\theta/\{B_p(\tfrac{3}{4}, \tfrac{1}{2})\}^{\frac{1}{3}}, \tag{20}$$

where $B_p(\frac{3}{4}, \frac{1}{2})$ is an incomplete Beta function (which is related to the binomial distribution function). The tables edited by Pearson (1934) span the required range of variables, and interpolation of the logarithms of entries is convenient. In evaluating the denominator of (19) it must be recalled that $0 \leqslant \theta \leqslant \pi$, and the integrand is an even function around $\theta = \frac{1}{2}\pi$, making the integral an odd function; once the integral has been evaluated from 0 to $\frac{1}{2}\pi$ the continuation is simple. The local heat transfer coefficient is a function of angle, as illustrated in figure 3. For a given direction of oscillation the maxima for the inner streaming transfer correspond to the minima of the corresponding outer streaming transfer coefficient distribution. For the inner streaming the average transfer coefficient is approximately 0·745 of the maximum local value.

When the analysis is carried through to render an equation for the average heat transfer in terms of the mean oscillation Reynolds number, $(a\omega d/\nu\sqrt{2})$, the result is

$$\overline{Nu} = 1{\cdot}36\, Re_{\text{osc}}^{\frac{1}{2}} Pr^{\frac{1}{3}}(a/R)^{\frac{1}{3}} H^{\frac{1}{3}}. \tag{21}$$

The heat transfer for flows outside the boundary-layer range can be described quite well by (21), especially since H does not vary very rapidly.

The calculation of laminar heat transfer at large Prandtl numbers can be extended down to moderate Prandtl numbers; the heat transfer can then be expressed in terms of a series in descending powers of the Prandtl number. On this basis, the right-hand side of (21) is to be divided by a series of which the leading terms are $\{1 + O(R/a)^{\frac{2}{3}} Pr^{-\frac{1}{3}}\}$.

An analysis for the inner streaming convection was attempted by Jameson (1964). As an approximation he dropped the term $v(\partial u/\partial y)$ from the boundary-layer energy equation so that the coefficient which he obtained is unreliable. It will be seen later that the result obtained here agrees much better with Jameson's experiments than his own analysis.

Regions of application of inner and outer streaming analysis

When the thermal boundary-layer thickness has increased in thickness to about one-half of the inner streaming region it runs into the thermal boundary layer which straddles the separating streamline, and it is no longer practicable to consider the problem by methods which are simply extensions of those used for $Pr \to \infty$. This means that for any $(\delta_{\text{a.c.}}/d)$ and Prandtl number there is a lower limit on (a/d) for which convection could be analysed on an inner streaming model as sketched above. Similarly, for the analysis based on the outer streaming,

when the temperature change across the conduction layer becomes as large as that in the outer streaming motion the scheme of analysis described earlier becomes inadequate; for any $(\delta_{a.c.}/d)$ and Prandtl number there is an upper limit on (a/d) for which the simple outer streaming analysis is applicable.

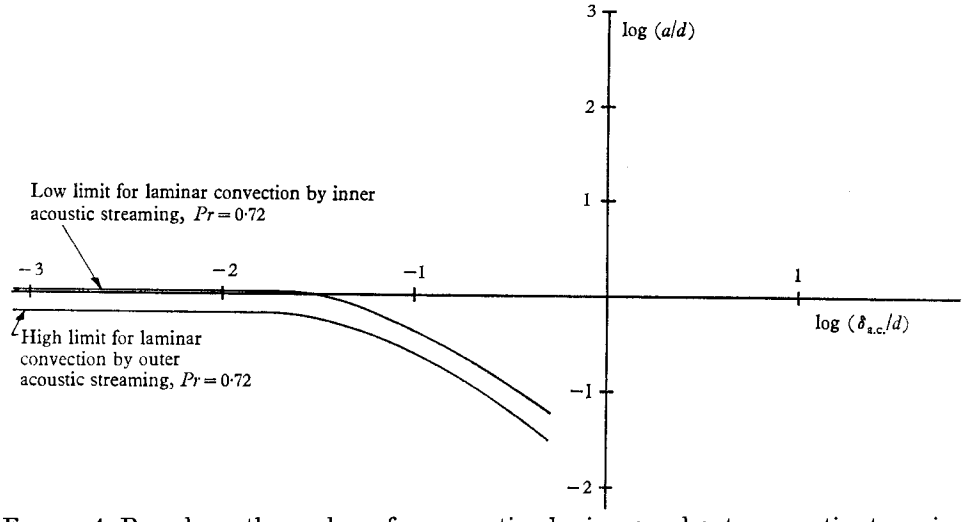

FIGURE 4. Bounds on the analyses for convection by inner and outer acoustic streaming for $Pr = 0{\cdot}72$. For an increase in the Prandtl (or Schmidt) number, the two lines should both be lowered in the (a/d) scale by a factor of $(Pr/0{\cdot}72)^{\frac{1}{2}}$. The lines at moderate $\delta_{a.c.}/d$ move down from the values for the thin boundary layer limit in accordance with the measurements of Raney *et al.* (1954).

The approximate positions of the lower bound for inner streaming analysis and the upper bound for outer streaming analysis are shown in figure 4 for $Pr = 0{\cdot}72$. For increases in Prandtl number, the bounds should be moved downwards by a factor of $Pr^{\frac{1}{2}}$. For flow in the boundary-layer analysis region, the bounds remain constant, but as $(\delta_{a.c.}/d)$ exceeds about 0·1 the inner streaming region becomes larger and the bounds both become progressively smaller. In illustrating this effect in figure 4 use was made of the measurements of Raney *et al.* (1954).

Fortunately there are no measurements which lie in the region between the two bounds, for which it would be necessary to develop a separate analysis. The only further analysis required before comparison is made with experiment is a modification of the outer streaming analysis appropriate for measurements where the streaming Reynolds number is large.

Convection by outer streaming at large Reynolds number

When the measurements in air at small a.c. boundary-layer thicknesses are considered it is clear that a large range of streaming Reynolds numbers is covered. When the streaming Reynolds number is large the outer streaming motion is confined to a boundary layer. This will give a smaller heat transfer rate than the corresponding case at small streaming Reynolds number, unless the Prandtl number is large enough for the thermal boundary to be considerably smaller than the boundary layer of the outer streaming motion. In some transitional range of

Reynolds numbers, between small and large values, the convection expected must decrease progressively from the low Reynolds number limit to the large Reynolds number limit.

Stuart (1966) presented a convenient analysis for the outer streaming boundary layer at large streaming Reynolds numbers. The flow warrants space and velocity transformations of its own; these can be chosen as

$$\left.\begin{aligned} 2\xi = x/R, \quad \zeta = za\omega/d(\omega\nu)^{\frac{1}{2}}, \\ V_0(\xi) = 2\sin 2\xi \quad \text{and} \quad \phi(\xi,\zeta) = \psi_{20}/a(\omega\nu)^{\frac{1}{2}}. \end{aligned}\right\} \tag{22}$$

Stuart demonstrates that the boundary-layer equation to be solved is

$$\frac{\partial\phi}{\partial\zeta}\frac{\partial^2\phi}{\partial\xi\,\partial\zeta} - \frac{\partial\phi}{\partial\xi}\frac{\partial^2\phi}{\partial\zeta^2} = \frac{\partial^3\phi}{\partial\zeta^3}. \tag{23}$$

When the outer flow boundary is considerably thicker than the a.c. boundary layer (to which the inner streaming is comparable in size), it is reasonable to use the outer behaviour of the Schlichting streaming solution as the inner boundary condition of the outer boundary layer, i.e. to put

$$\frac{\partial\phi}{\partial\zeta} = X(\xi), \quad \phi = 0 \quad \text{at} \quad \zeta = 0, \tag{24}$$

where the thickness of the inner streaming motions is ignored and where

$$X(\xi) = -\tfrac{3}{4}V_0\frac{dV_0}{d\xi}, \tag{25}$$

which is a transformed equivalent of (6). The outer boundary condition is

$$\frac{\partial\phi}{\partial\zeta} \to 0 \quad \text{as} \quad \zeta \to \infty. \tag{26}$$

A solution to (23) can be sought in the form

$$\phi = \gamma(\xi) + \epsilon\phi_1(\xi,\zeta) + \epsilon^2\phi_2(\xi,\zeta) + \ldots. \tag{27}$$

The arbitrary quantity ϵ is an escalating order parameter such that, after (27) has been substituted in (23), equations containing terms of the same order can be separated and solved successively. This process leaves $\gamma(\xi)$ undetermined, but when the functions $\phi_1, \phi_2, \ldots$ are substituted back into (27) with ϵ set equal to unity an ordinary differential equation for γ is found, and a series solution obtained. If

$$X(\xi) = m^2\xi(1 + \beta_2\xi^2 + \beta_4\xi^4 + \ldots), \tag{28}$$

the solution for γ can be written

$$\gamma(\xi) = m\xi\left\{1 + \tfrac{3}{17}\beta_2\xi^2 + \left[\frac{6201}{1{,}116{,}985}\beta_2^2 + \tfrac{60}{773}\beta_4\right]\xi^4\ldots\right\} \tag{29}$$

and for ϕ_n:

$$\phi_1 = -X\left[\frac{1}{\gamma'}\right]e^{-\gamma'\zeta}, \tag{30}$$

$$\phi_2 = X^2\left[\frac{\gamma''}{2\gamma'^4}\right]\{e^{-\gamma'\zeta} - \tfrac{1}{2}e^{-2\gamma'\zeta}\}. \tag{31}$$

The leading term for the u-component of velocity is found as

$$\partial\phi_1/\partial\zeta = X e^{-\gamma'\zeta}. \tag{32}$$

$(\partial\phi_n/\partial\zeta) = 0$ at $\zeta = 0$ for $n > 1$, and the velocity corrections which these ϕ_n introduce relative to (32) have their largest magnitude at finite ζ. As such, they have a smaller influence in the computation of convection than they would if their magnitudes were finite at $\zeta = 0$. Thus (32) is an acceptable approximation for use in estimating heat convection. Moreover, in the vicinity of a forward stagnation point

$$\partial\phi/\partial\zeta = m^2\xi e^{-m\zeta} \tag{33}$$

is an exact solution of the equation. For a circular cylinder, $m = 2\sqrt{3}$. With this relation, it is possible to estimate the heat transfer in the stagnation region by standard techniques. The boundary-layer energy equation can be integrated numerically for $Pr = 0{\cdot}72$ to yield a value of $0{\cdot}462$. A further estimate can be found, which is an explicit function of Prandtl number, by the Meksyn–Merk technique. The results of these methods are in close agreement, as might be expected, and should be compared with the value of $hR(3\nu/\omega)^{\frac{1}{2}}/ka$ obtained when Re_s is small; this value is $(0{\cdot}72)^{\frac{1}{2}}(2/\pi)^{\frac{1}{2}}$, i.e. $0{\cdot}685$. It is seen immediately that at this Prandtl number, the heat transfer is significantly reduced at large Re_s in the regions where the outer streaming flow has forward stagnation points.

It is desirable to calculate the local heat transfer distribution around the cylinder from the stagnation points to the separation points when Re_s is large. For the corresponding case when Re_s is small, it was found that the conduction thickness, k/h, is proportional to $\sec(x/R)$. It may be expected that a similar dependence upon (x/R) would be found for large Re_s if the local value of $1/\gamma'$ also corresponds to $\sec(x/R)$, since this would maintain a constant ratio of boundary-layer thicknesses around the cylinder. If, however, γ' remained effectively constant around the cylinder, the local ratio of the thermal boundary-layer thickness to the velocity thickness would progressively increase, and this would lead to local heat transfer coefficients which are smaller than $\cos(x/R)$ times the stagnation point value. The actual situation lies somewhere between these extremes, but with the present state of knowledge of the flow field it is difficult to determine it precisely. The difficulty lies in the convergence of the series for γ', derived from equation (29). It will be sufficient for comparison with experiments presently available to observe that an upper limit, at large Re_s, for $Pr = 0{\cdot}72$ is

$$\overline{Nu}R\left\{1 + 0{\cdot}95\frac{a}{d}\right\}\Big/ Re_{\mathrm{osc}}(3\nu/\omega)^{\frac{1}{2}}Pr^{\frac{1}{2}} = 0{\cdot}484. \tag{34}$$

4. Comparison with experiments

The analyses described in the previous section do not take any account of natural convection. The latter is always present to some degree in laboratory experiments. To compare analysis and experiment, it is sometimes necessary to extrapolate the observed behaviour to try to eliminate the influence of natural convection effects. Such extrapolation is not necessary in every case here for the

basic agreement between analysis and experiment to be established; it is required principally for the sets of measurements made in air with small boundary-layer thicknesses.

Convection by outer streaming at small streaming Reynolds numbers

The smallest streaming Reynolds numbers are found in the investigations at higher frequencies in air; these include the measurements of Fand & Kaye (1961*a*) and Lee & Richardson (1965). In these investigations natural convection

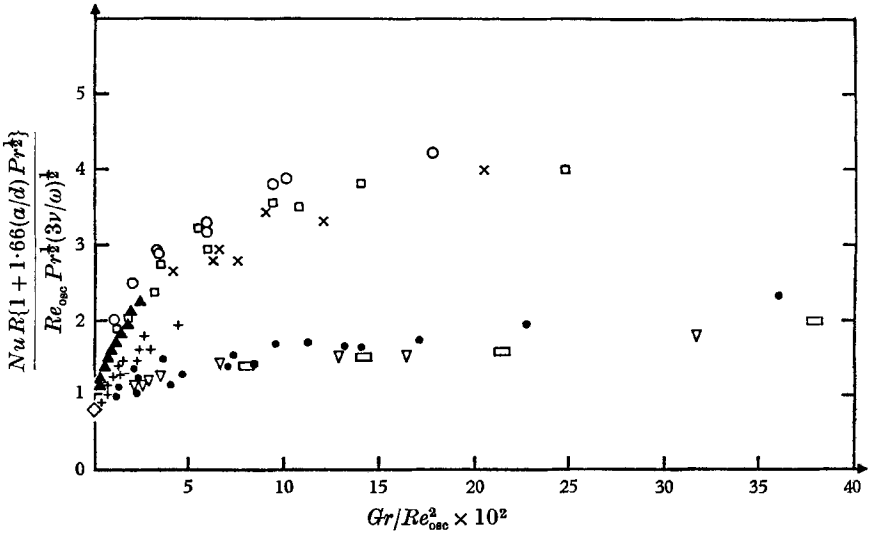

FIGURE 5. Comparison of analysis for convection by outer streaming at small streaming Reynolds numbers with experiment. The 'target' derived from analysis is shown as a diamond-shaped point. To avoid crowding, some data points have been omitted. Lee & Richardson (1965): 645, ▽; 627, □; Fand & Kaye (1961*a*); 1101, ●; 1496, +; 2116, ▲; 2942, □; 3378, ○; 4872, ×.

had significant effects; indeed, the investigations might be considered as studies principally of natural convective flow perturbed by sound fields rather than vice versa. From equation (16), it is expected that the quantity

$$\overline{Nu}R\left\{1+1{\cdot}66\frac{a}{d}Pr^{\frac{1}{2}}\right\}\Big/Re_{osc}Pr^{\frac{1}{2}}(3\nu/\omega)^{\frac{1}{2}}$$

attains the value of 0·718 in the limit as Grashof number tends to zero. This quantity is plotted as a function of the ratio of Grashof number to the square of the oscillation Reynolds number in figure 5. It can be seen clearly in this graph that the data do indeed tend to the vicinity of the expected value in the limit. This provides affirmation of the analysis for a considerable variation in frequency.

Convection by inner streaming

Measurements which qualify exceptionally well for analysis by inner streaming are the mass transfer measurements of Jameson (1964); benzoic acid cylinders were oscillated in a glycerol–water solution, entailing a Schmidt number of

about 3×10^7. These measurements were made in a region where the inner streaming flow is larger in extent than that predicted by boundary-layer analysis. When the interface area between inner and outer streaming is relatively large compared with the cylinder surface the resistance to mass transport across the separating streamlines may play a relatively minor role in the convective process. The data presented by Jameson have been plotted together with a line for equation (21) with $H = 1$ on figure 6. It can be seen that the data lie parallel to the prediction given by this equation, with the average of the points lying a little below the value expected if there were no resistance to transport into the outer bulk of the fluid.

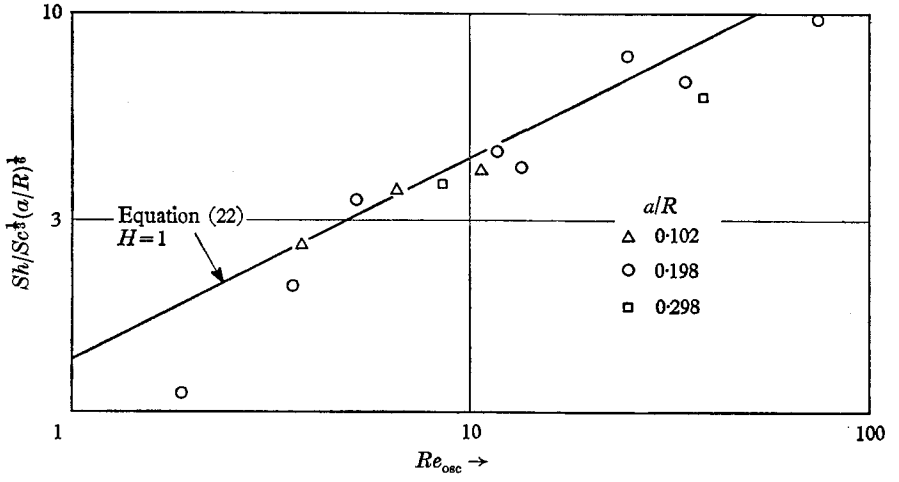

FIGURE 6. Comparison of analysis for convection by inner streaming with Jameson's (1964) measurements at large Schmidt number.

A typical value for H can be estimated from the work of Holtsmark *et al.* (1954) corresponding say, to a value of $\log(\delta_{a.c.}/d)$ of $-0{\cdot}77$, typical of these experiments; the value of H has an insignificant difference from unity. This seems to be a more satisfactory result than in the comparison made by Jameson, where the approximate solution lay considerably lower than the measurements. Jameson noted that his omission of a term in his approximate solution would give a conservative estimate.

The measurements of Rao *et al.* (1963) involve a smaller Schmidt number than Jameson's work, and also larger maximum values of (a/d). However, the results follow the trend of the analysis very well and are of the order of 50–70 % of expectation from equation (21). An overestimation can be expected since (21) accounts only for the resistance to transport at the cylinder surface and is based on an analysis for small (a/d). This point is discussed more extensively for the data of Lemlich & Rao (below).

The other data which can be compared with analysis for convection by inner streaming are those of Lemlich & Rao. For the measurements made in air, the published work does not present sufficient details concerning the amplitude and frequency for each data point to permit a direct comparison. The measurements of Lemlich & Rao (1965) for a cylinder oscillated in liquids are described in

sufficient detail for a comparison to be made. However, there is some question as to whether a comparison with the present analysis is adequate, since the measurements involve values of (a/d) of around unity, while the flow analysis was built upon an expansion of the stream function in terms of orders increasing successively by a factor of (a/d). Further, it is expected that for these measurements the ratio of the inner thermal boundary-layer thickness to the inner streaming boundary-layer thickness is much larger than the ratio of the concentration boundary-layer thickness to the inner streaming boundary-layer thickness in the work of Jameson. This would tend to make the asymptotic analysis

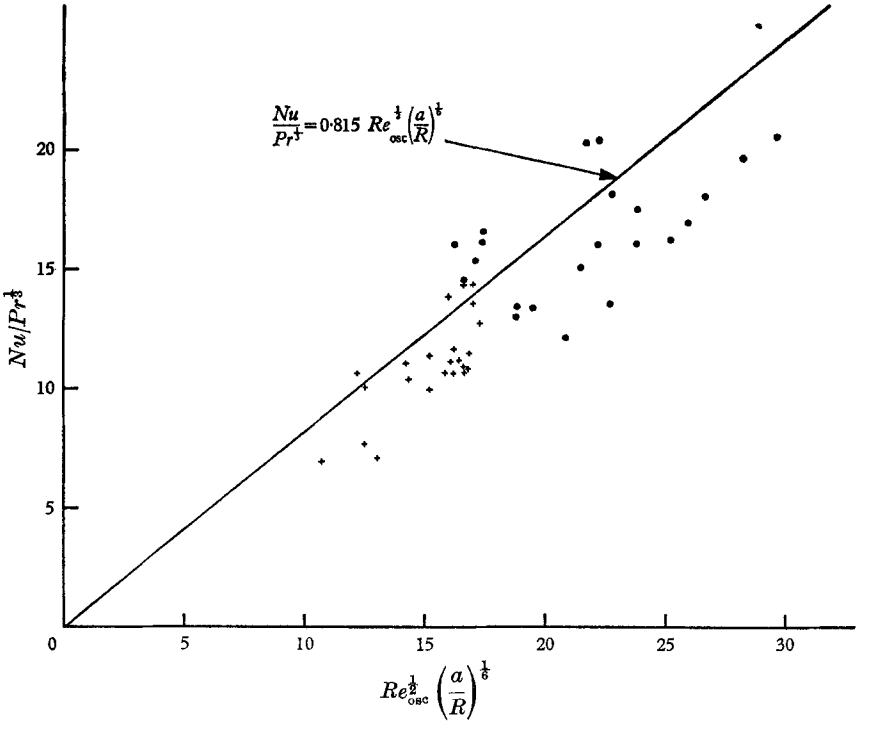

FIGURE 7. Comparison of analysis for convection by inner streaming with Lemlich & Rao's (1965) measurements at moderate Prandtl number. The solid line corresponds to 60 % of expectation from equation (21).

overestimate the heat transfer and to make the resistance to transport across the dividing streamline relatively more important. Under these circumstances, it might be reasonable to accept a correlation of the heat transfer if it displayed the right form of dependence of heat transfer upon the parameters contained within (21), with the numerical coefficient representing an overall resistance to heat transport which is perhaps 2 to 3 times the resistance of the innermost thermal layer by itself. The results of Lemlich & Rao are displayed in figure 7, where it can be seen that the results do indeed follow the trend predicted by the equation and have an average coefficient within acceptable limits. It is difficult to identify a definite influence of Grashof number in these results, and there have been no adequate studies of local details of the flow at finite Grashof numbers.

Convection by outer streaming at large streaming Reynolds numbers

Amongst the measurements in air the results of Fand & Kaye (1961*b*) and of Fand & Peebles (1962) are most suited to comparison with analysis for convection by outer streaming at large streaming Reynolds number. The results for vertical oscillations at 97·5 c/s and horizontal oscillations at 104 c/s are shown on figure 8, where the convection number from equation (34) is plotted as a function of Gr/Re_{osc}^2. For measurements represented in this graph the streaming Reynolds numbers range from about 75 to 550, the larger being closer to the convection-number axis. On figure 8 it can be seen that the results extrapolate to a value a little below the expected upper limit of 0·484. This graph demonstrates excellent agreement with analysis.

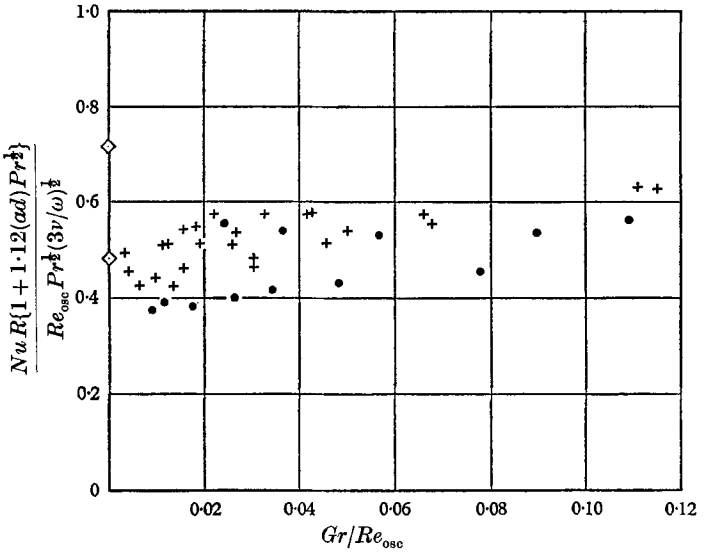

FIGURE 8. Comparison of analysis for convection by outer streaming at large streaming Reynolds numbers with experiment. The target point of approximately 0·484, from equation (34), is the lower diamond on the axis. The expectation for small streaming Reynolds numbers is shown as the upper diamond on the axis. +, Fand & Kaye (1961*b*), vertical oscillations 97·5 c/s; ●, Fand & Peebles (1962), horizontal oscillations 104 c/s.

The results of Martinelli & Boelter (1938) were also obtained at large streaming Reynolds numbers. Numerical solution at the stagnation point with $Pr = 5{\cdot}0$ leads to a dimensionless temperature gradient at the wall of 1·55, which can be compared to the value of $(10/\pi)^{\frac{1}{2}} = 1{\cdot}78$ given for the corresponding quantity by the analysis for small streaming Reynolds numbers. This results in an upper bound for $\overline{Nu}/Re_{osc}$ of about 0·011, which compares favourably with figure 7 of Martinelli & Boelter, where the ratio $\overline{Nu}/Re_{osc}$ has a value of about 0·009 for $2\times10^3 < Re_{osc} < 8\times10^3$. This is a satisfactory correspondence, especially when it is realized that the experiments were performed in water, a fluid with transport properties significantly different from those of air. The theory is vindicated by results from both fluids.

In figures 5 and 8 the ratio of Grashof number to the square of Reynolds number

has been formed using the oscillation Reynolds number rather than the streaming Reynolds number. This usage has no significance or importance other than convenience.

5. Discussion

The analysis of the effects of oscillations and vibrations presented here has omitted the contribution of buoyancy forces. When buoyancy forces are considered in addition to the oscillatory flow, some additional parameters arise: these include the ratio λ of the natural convection length scale, $R/Gr^{\frac{1}{4}}$, to the a.c. boundary-layer thickness, $(\nu/\omega)^{\frac{1}{2}}$; and Re_{osc}^2/Gr. The solutions obtained here should be the asymptotic solutions (as $Re_{\mathrm{osc}}^2/Gr \to \infty$) for the more general problem. Thus, for small Re_s and $\lambda \to \infty$ the asymptotic solution should correspond to equation (13). The solutions for this more general problem are beyond the scope of the present paper, but are in the process of computation and will be reported later. The major purpose of this paper has been to put convection by acoustic streaming into perspective and to examine the analysis of the various asymptotic examples for a circular cylinder. It has been found that there is very satisfactory agreement with experiment throughout.

A further generalization of the analysis can readily be seen for body shapes other than the circular cylinder. The acoustic streaming on a cylinder is a steady flow generated by Reynolds stresses. These Reynolds stresses correspond to spatial gradients of the time-average products of the fluctuating velocity components. They can be found in unsteady flow over body shapes other than the circular cylinder. For cases where the wavelength of propagation of oscillations is small compared with the body size, the necessary gradients can occur even on a flat surface. Thus it is possible for acoustic streaming to occur in geometries other than the circular cylinder, and the analysis of convection can be extended to these geometries. For bodies which are immersed in a fluid and undergo oscillations having a wavelength large compared with their size, the first-order flow is computed with the aid of the potential-flow solution for the corresponding steady flow problem. In this way, an unexpected use is found for some classical analyses of potential flow.

It would be useful to investigate the hydrodynamic stability of the flow, and also to investigate further the flow and heat transfer processes in the neighbourhood of the separating streamline for the case of convection by inner streaming.

It is very desirable that studies of the effects of oscillations combined with buoyancy should be carried further, because these will permit detailed comparison with experimental data for local heat transfer already available, and techniques will be developed for analysis of other cases where oscillations are imposed upon an independently-driven flow. A case of special interest is the flow in the forward stagnation region of a bluff body, where oscillations are generated by a Kármán street. The oscillation intensity experienced on the cylinder can be increased markedly by the application of disturbances in the flow (Gerrard 1965), so that it may be possible to explain part of the sensitivity of stagnation-point heat transfer to free-stream turbulence in this way. Another case of inter-

est which may yield to analysis using some of the viewpoints developed here is the liquid-phase convection in nucleate pool boiling, where it is known that large oscillations occur and can contribute a significant part of the total heat transfer from the surface.

The suggestion that heat transfer is due to acoustic streaming is not new in itself. The closest that a previous study has come to the analysis described here is probably represented by some investigations where a sound field was propagated axially along a heated circular cylinder (e.g. Kubanskii 1962). In the framework of the present paper, Kubanskii's work was related to an initial influence study for average heat transfer (Re^2_{osc}/Gr small), and did not include the case of $Re^2_{osc}/Gr \to \infty$ which forms the main topic here.

The author is grateful to Prof. J. T. Stuart for his kindness in making available a copy of his manuscript on acoustic streaming at large streaming Reynolds numbers before its publication in the *Journal of Fluid Mechanics*. Mr Robert Kocsis, graduate student at Brown University, assisted by performing many computations and preparing some of the figures.

The work described in this paper constitutes part of a research program on heat transfer in unsteady flows of the Aerospace Research Laboratories, Office of Aerospace Research of the U.S. Air Force, under the technical cognizance of Dr M. Scherberg. This support is gratefully acknowledged.

REFERENCES

EVANS, H. L. 1962 *Int. J. Heat Mass Transfer*, **5**, 35.

FAND, R. M. & KAYE, J. 1961*a* *Trans. Am. Soc. Mech. Engrs, J. Heat Transfer*, **83**, 133.

FAND, R. M. & KAYE, J. 1961*b* *Int. Developments in Heat Transfer (Proc. 2nd Int. Conf.)*, Part 11, 490.

FAND, R. M. & PEEBLES, E. M. 1962 *Trans. Am. Soc. Mech. Engrs, J. Heat Transfer*, **84**, 268.

GERRARD, J. H. 1965 *J. Fluid Mech.* **22**, 187.

HOLTSMARK, J., JOHNSON, I., SIKKELAND, T. & SKAVLEM, S. 1954 *J. Acoust. Soc. Am.* **26**, 102.

JAMESON, G. J. 1964 *Chem. Engng Sci.* **19**, 793.

KUBANSKII, P. N. 1962 *Akust. Zhur.* **8**, 85.

LEE, B. H. & RICHARDSON, P. D. 1965 *J. Mech. Engng Sci.* **7**, 127.

LEMLICH, R. & RAO, M. A. 1965 *Int. J. Heat Mass Transfer*, **8**, 27.

MARTINELLI, R. C. & BOELTER, L. M. K. 1938 *Proc. 5th Intl. Congr. Appl. Mech.* 578.

MEKSYN, D. 1961 *New Methods in Laminar Boundary-Layer Theory*. Oxford: Pergamon.

MERK, H. J. 1959 *J. Fluid Mech.* **5**, 460.

PEARSON, K. 1934 *Tables of the Incomplete Beta Function*. London: Biometrika.

RANEY, W. P., CORELLI, J. C. & WESTERVELT, P. J. 1954 *J. Acoust. Soc. Am.* **26**, 1006.

RAO, K., RAJU, S. & RAO, C. V. 1963 *Indian Chem. Engr.* **5**, 100.

RICHARDSON, P. D. 1964 *J. Acoust. Soc. Am.* **36**, 2323.

RICHARDSON, P. D. 1966 *Proc. 3rd Intl. Heat Transfer Conf.* **3**, 71.

RICHARDSON, P. D. 1967 *Appl. Mech. Rev.* **20**, 201.

ROSENHEAD, L. 1963 (Ed.) *Laminar Boundary Layers*. Oxford University Press.

SCHLICHTING, H. 1932 *Z. Phys.* **61**, 349.

STUART, J. T. 1963 see Rosenhead (1963).

STUART, J. T. 1966 *J. Fluid Mech.* **24**, 673.